RESEARCH ARTICLE

miRNAs may play a major role in the control of gene expression in key pathobiological processes in Chagas disease cardiomyopathy
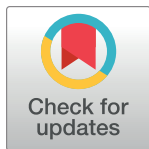
Laurie Laugier[1☺], Ludmila Rodrigues Pinto Ferreira[2,3,4☺], Frederico Moraes Ferreira[2,3,4☺], Sandrine Cabantous[1], Amanda Farage Frade[2,3,4], Joao Paulo Nunes[2,3,4], Rafael Almeida Ribeiro[2,3,4], Pauline Brochet[5], Priscila Camillo Teixeira[2,3,4], Ronaldo Honorato Barros Santos[6], Edimar A. Bocchi[6], Fernando Bacal[6], Darlan da Silva Cândido[2,3,4], Vanessa Escolano Maso[7], Helder I. Nakaya[7,8], Jorge Kalil[2,3,4], Edecio Cunha-Neto[2,3,4‡]*, Christophe Chevillard[5‡]*

1 Aix Marseille Université, Génétique et Immunologie des Maladies Parasitaires, Unité Mixte de Recherche S906, Marseille, France; INSERM, U906, Marseille, France, 2 Laboratory of Immunology, Heart Institute (InCor), University of São Paulo, School of Medicine, São Paulo, Brazil, 3 Division of Clinical Immunology and Allergy, University of São Paulo, School of Medicine, São Paulo, Brazil, 4 Institute for Investigation in Immunology (iii), INCT, São Paulo, Brazil, 5 Aix Marseille Université, TAGC Theories and Approaches of Genomic Complexity, Inserm, INSERM, UMR_1090, Marseille, France, 6 Division of Transplantation, Heart Institute (InCor), University of São Paulo, School of Medicine, São Paulo, Brazil, 7 Department of Pathophysiology and Toxicology, School of Pharmaceutical Sciences, University of São Paulo, São Paulo, Brazil, 8 Scientific Platform Pasteur, University of São Paulo, São Paulo, Brazil

☺ These authors contributed equally to this work.
‡ ECN and CC also contributed equally to this work.
* edecunha@gmail.com (ECN); christophe.chevillard@univ-amu.fr (CC)

Abstract

Chronic Chagas disease cardiomyopathy (CCC), an especially aggressive inflammatory dilated cardiomyopathy caused by lifelong infection with the protozoan *Trypanosoma cruzi*, is a major cause of cardiomyopathy in Latin America. Although chronic myocarditis may play a major pathogenetic role, little is known about the molecular mechanisms responsible for its severity. The aim of this study is to study the genes and microRNAs expression in tissues and their connections in regards to the pathobiological processes. To do so, we integrated for the first time global microRNA and mRNA expression profiling from myocardial tissue of CCC patients employing pathways and network analyses. We observed an enrichment in biological processes and pathways associated with the immune response and metabolism. IFNγ, TNF and NFkB were the top upstream regulators. The intersections between differentially expressed microRNAs and differentially expressed target mRNAs showed an enrichment in biological processes such as Inflammation, inflammation, Th1/ IFN-γ-inducible genes, fibrosis, hypertrophy, and mitochondrial/oxidative stress/antioxidant response. MicroRNAs also played a role in the regulation of gene expression involved in the key cardiomyopathy-related processes fibrosis, hypertrophy, myocarditis and arrhythmia. Significantly, a discrete number of differentially expressed microRNAs targeted a high number of differentially expressed mRNAs (>20) in multiple processes. Our results suggest that miRNAs orchestrate expression of multiple genes in the major pathophysiological

processes in CCC heart tissue. This may have a bearing on pathogenesis, biomarkers and therapy.

Author summary

Chronic Chagas disease cardiomyopathy (CCC), an aggressive dilated cardiomyopathy caused by *Trypanosoma cruzi*, is a major cause of cardiomyopathy in Latin America. Little is known about the molecular mechanisms responsible for its severity. Authors study the possible role of microRNAs in the regulation of gene expression in relevant pathways and pathobiological processes. Differentially expressed genes (DEGs) and differentially expressed miRNAs (DEMs) -small RNAs that can regulate gene expression—associated to severe cardiomyopathy development. The inflammatory mediator Interferon-γ was the most likely inducer of gene expression in CCC, and most genes belonged to the immune response, fibrosis, hypertrophy and mitochondrial metabolism. A discrete number of differentially expressed mRNAs targeted a high number of differentially expressed mRNAs in multiple processes. Moreover, several pathways had multiple targets regulated by microRNAs, suggesting synergic effect. Results suggest that microRNAs orchestrate expression of multiple genes in the major pathophysiological processes in CCC heart tissue.

Introduction

Chagas disease is a major public health problem in Latin America, resulting from lifelong infection with the protozoan parasite *Trypanosoma cruzi*. Up to 30 years after acute infection, approximately 30% of the 6 million infected people eventually develop chronic Chagas cardiomyopathy (CCC), a life-threatening inflammatory dilated cardiomyopathy [1,2]. Most other *T. cruzi*-infected patients will remain asymptomatic for life (60%) or develop digestive disease, which causes less deaths (approx. 10%) [1]. Chagas disease is the most common cause of non-ischemic cardiomyopathy in Latin America, causing approximately 10,000 deaths/year, mainly due to heart failure and severe arrhythmia/sudden death [1]. Migration turned Chagas disease into a global health problem, with an estimated 400,000 infected persons living in nonendemic countries, mainly the United States and Europe. Current anti–*T. cruzi* drugs have shown to be unable to block progression toward CCC [3].

After acute infection, parasitism is partially controlled by the immune response, and low-grade parasite persistence fuels the systemic production of inflammatory cytokines like IFN-γ and TNF-α, which is more intense in CCC than ASY patients [4–6]. CCC is characterized by a monocyte and T cell-rich myocarditis [7,8] with cardiomyocyte damage and hypertrophy, and prominent fibrosis; *T. cruzi* parasites are very scarce. IFN-γ producing Th1 cells accumulate in the myocardium of CCC patients [4,9,10] in response to locally produced chemokine ligands CXCL9 and CCL5 [11]. Accordingly, IFN-γ was found to be the most highly expressed cytokine mRNA in CCC myocardium using a 13-cytokine panel [12]. Both heart-crossreactive [13] and *T. cruzi*-specific T cells [14] have been found in CCC heart tissue, and both and may play a role in the myocarditis of CCC. Together, evidence suggests that myocarditis and IFNγ signaling plays a major pathogenic role in CCC development and severity (reviewed in [2,15]), although downstream events leading to the heart disease phenotype are still obscure.

CCC has a worse prognosis than cardiomyopathies of non-inflammatory etiology, like ischemic or idiopathic dilated cardiomyopathy (DCM) [15]. Our group has shown that the myocardial gene expression profiles in CCC patients are profoundly different from those of both heart donors and DCM patients as assessed the "Cardiochip" cDNA microarray encoding ca. 11,000 expressed sequence tags (EST) cDNAs expressed in cardiovascular tissue [16]. Indeed, 15% of all genes specifically upregulated in CCC myocardium were found to be IFN-γ-inducible, indicating a strong IFN-γ transcriptional signature. This suggested that the increased aggressiveness of CCC could be related at least in part to activation of IFN-γ-dependent genes and pathways. Significantly, systemic overexpression of IFNγ in transgenic mice causes a TNFα-dependent inflammatory dilated cardiomyopathy [17,18]. Likewise, immuno-histological signs of inflammation in suspected myocarditis of postviral etiology is associated with a poor prognosis [19], and sustained and long-term inflammation plays a role in worsening cardiac hypertrophy and chronic heart failure [20]. Mitochondrial dysfunction and oxidative stress have been associated with the pathogenesis of dilated cardiomyopathy and heart failure [21,22]. Indeed, our group has observed altered levels of 16S mitochondrial RNA as well as mRNA encoding mitochondrial proteins [16] and reduced levels of mitochondrial energy metabolism enzymes in that were specific to CCC [23]. Myocardial mitochondrial dysfunction and oxidative stress have been identified and explored in murine models of CCC (Reviewed in [24]). However, the determinants of expression of the majority of differentially expressed genes in CCC- as well as their roles in the key pathogenic roles of hypertrophy, fibrosis, arrhythmia and myocarditis—still remained mostly unknown.

MicroRNAs (miRNAs), short non-coding RNAs (18 to 24 nucleotides), are post-transcriptional regulators critically involved in a multitude of biological processes by modulating protein expression of up to 60% of the genes. miRNAs act by hybridizing with complementary sequences the 3'untranslated region (UTR) of mRNAs, exerting a downregulatory effect through direct degradation of the target mRNA and/or translational repression. MiRNAs also play a key role in multiple disorders, including cardiovascular disease [25]. Modulation of miRNA expression can profoundly alter disease phenotypes, and miRNA-based therapeutics has already entered clinical trials [26]. Our group recently studied the mRNA and miRNA transcriptome in the myocardium of mice acutely infected by *T. cruzi* [27], and we have previously shown that expression of muscle-enriched miRNAs ("myoMiRs", including miR-1 and miR-133) is downmodulated in CCC myocardium, suggesting miRNA may control expression of pathogenetically relevant genes in CCC [28]. We raised the hypothesis that mRNA expression and pathways/processes may to be heavily influenced by miRNA expression. To comprehensively address this issue, we performed an integrative genome-wide analysis of the role of miRNA in global gene expression in CCC.

Methods

Ethics statement

The protocol was approved by the Institutional Review Board of the University of São Paulo, School of Medicine and written informed consent was obtained from the patients. All experimental methods comply with the Helsinki declaration.

Patients and sample collection

Human left ventricular free wall heart tissue was obtained from end-stage heart failure patients at the moment of heart transplantation. Patients with CCC presented positive *T. cruzi* serology and typical heart conduction abnormalities (right bundle branch block and/or left anterior division hemiblock) and had a histopathological diagnosis of myocarditis, fibrosis and

hypertrophy. Left ventricular free wall samples were also obtained from hearts of organ donors, which were not used for transplantation due to size mismatch with available recipients. (n = 4) All left ventricular free wall heart tissue samples were cleared from pericardium and fat and quickly frozen in liquid nitrogen and stored at −80°C.

RNA Extraction and RT-PCR

Myocardium samples (20–30 mg) were crushed with ceramic beads (CK14, diameter 1.4 mm) in 350 μl of RLT lysis buffer supplemented with 3.5 μl of β-mercapto-ethanol. Total RNA for mRNA expression profiling was extracted with the RNeasy Mini Kit (Qiagen, Courtaboeuf, France) adapted with Trizol. RNA quality and quantity was measured with a 2100 Bioanalyser. Total RNA (1μg), with a RIN > 7, was reverse-transcribed with the high Capacity cDNA Reverse Transcription Kit (ThermoFisher Scientific, Saint Aubin, France).

Whole human genome expression analysis

Whole genome expression analysis was done on SurePrint G3 Human GeneExpression v1 8x60K arrays (Agilent Technologies, Les Ulis, France) following the manufacturer's protocol. Gene expression data were previously deposited in the GEO database (GSE84796 and GSE111544). Microarray analyses and signal normalization were done with GeneSpring software (11.5.1), T test with adjustment for false discovery rate with the Benjamini-Hochberg method. Genes were considered differentially expressed if adjusted P values were <0.05 and absolute fold change >2.0. In order to validate the microarray results, quantitative real-time PCR, from 20ng of cDNA, was performed with the ABI 7900HT thermocycler and TaqMan Universal PCR Master Mix (Applied Biosystems, Life Technologies). The Student's T test was used to identify differentially expressed genes between CCC and controls by TaqMan RT-qPCR. Gene expression data used in this manuscript are the same ones that used in one of previous work on methylation analysis.

Principal component analysis, network and pathways analysis

Principal component analysis (PCA) analysis was performed using all differentially expressed genes and the variance expression of the number of standard deviations from mean overall samples. Canonical pathways analysis, networks analysis and Upstream regulator analysis, and classification of differentially genes belonging to pathways and biological processes were performed with Ingenuity Pathway Analysis (IPA, Qiagen Redwood City, CA, USA). We also classified genes in additional relevant pathobiological processes and pathways such as inflammation, IFNγ-modulated genes/Th1 response, extracellular matrix, fibrosis, hypertrophy, contractility of heart, hypertrophy, arrhythmia, oxidative stress/antioxidant response, mitochondria, and mitochondria-related genes using IPA Knowledge Base (IKB) gene lists, which were in some cases merged with other published gene lists. The IFNγ-dependent/Th1 response gene list was merged with published IFNγ-induced/repressed gene lists [29], and the oxidative stress gene list was merged with Nrf2-modulated genes [30]. The NF-kB-modulated gene list was obtained from Yang et al. [31]. The mitochondrial gene list was a combination of all genes contained in the Mitochondrion Gene Ontology term and Mitocarta 2.0 [32]. Deconvolution of immune and cardiac cell types was performed by comparing the differentially expressed genes with the ARCHS4 tissue database in the EnrichR tool [33] (Adjusted P-value < 0.001). The network of cell types representing the genes shared by different tissues was constructed using the Cytoscape tool [34]. Prediction of differentially expressed miRNA-mRNA target relationships was performed with the IPA Knowledge Base. We selected high predicted or experimentally validated miRNA-target relationships.

Quantitative miRNA expression profiling

RNA and cDNA were obtained from human myocardial samples as previously described [35]. MiRNA profiling experiments were done for 754 miRNAs using pre-printed TLDA microfluidic cards (Human MicroRNA Card Set v3.0), according to the manufacturer's protocols and as described [35]. Raw TLDA data files were pre-processed with threshold and baseline corrections for each sample (automatic baseline and threshold set to 0.3) with assessment of each amplification plot on SDS 2.3 software (ThermoFisher). Cycle threshold (Ct) values from quantitative real time PCR data were imported, normalized and tested for statistical significance with the HTqPCR Bioconductor package [36]. Samples data quality and outliers removal were assessed with the arrayQualityMetrics Bioconductor package [37]. Distribution of the samples Ct values were normalized against the endogenous control RNU48-001006. Differentially expressed miRNAs (DEMs) were determined using a wrapper function from the Bioconductor package LIMMA [38]. Variance filtering was applied and, for each miRNA, up to two failed reads per group were accepted for partial coefficients calculation. Resulting p-values were submitted to false discovery rate adjustment according to the Benjamini-Hochberg method and the statistical significance threshold was defined as p-value ≤ 0.05, with an absolute fold change cutoff ≥ 1.5.

miRNA target gene interaction analysis

miRNA-target gene interaction analysis was done with performed with Ingenuity Pathway Analysis (IPA, Qiagen Redwood City, CA, USA). Analysis was done in three steps. First of all, for each DEM, we extracted from IPA database all the reported target genes (high predicted or experimentally observed). Then, among all these targets we kept only the ones that were differentially expressed (DEGs) in our gene expression analysis. Finally, we kept only the targets presenting an inverse pairing expression. In the analysis we included DEMs with an absolute fold change over 1.5 and DEGs with an absolute fold change over 2.0.

Results

Information on the subjects studied in this paper is available in **Table 1**

We found 1535 genes to be differentially expressed (DEG) between CCC and control myocardium, of which 1105 (72%) are upregulated, while 430 (28%) genes are downregulated in CCC (**S1 Table**). To validate the microarray results, we performed qPCR of 44 differentially expressed genes on the same samples (independent extractions) used for the microarray study, plus 16 new CCC samples. The confirmation rate was 86%, and only for 6 genes (ABRA, CDC42, ESRRA, GPD1, NFATC2, TGFBR2), the expression patterns were not confirmed. The gene specific qRT-PCR results, including fold change and p values, were previously described ([39], S2 Table).

A PCA analysis based on the all differentially expressed genes (DEGs) showed clustering of samples from each group in distinct areas of the plot (**Fig 1A**), confirming that CCC myocardial gene expression patterns were substantially different from controls. A heatmap based on DEGs confirmed the good clustering (**S1A Fig**). Likewise, differential clustering of CCC and control miRNAs also confirmed miRNA expression patterns are distinct in CCC and controls (**Fig 1B**). IPA canonical pathways analysis showed that the most enriched pathways are mainly immune-related, such as Th1 and Th2 T cells, dendritic cells/antigen presentation, leukocyte extravasation, NK and B cells; this is consistent with the high number of upregulated genes from the incoming inflammatory cells present in CCC but not in control heart tissue (**Fig 2A**). **S2 Table** depicts the DEGs belonging to all significant IPA canonical pathways. **Fig 2B** shows the number of genes in each pathobiological process relevant for the disease such as

Table 1. Characteristics of the human left ventricular free wall heart tissue samples used in this study.

Project Number	Form	EF	Age	Sex	Transcriptome Analysis	qRT-PCR validation	MiRnome Analysis
EBS	CCC	0.12	32	M	x	x	x
NSR	CCC	0.15	49	F	x	x	
MGS	CCC	0.20	61	F		x	
BHAN	CCC	0.20	15	M		x	
SCS	CCC	0.17	59	M	x	x	x
ECA	CCC	0.19	32	F		x	
VTL	CCC	0.19	41	M		x	
APA	CCC	0.20	60	F	x	x	
MCRS	CCC	0.20	45	F	x	x	x
MERS	CCC	0.20	39	F		x	
MSS	CCC	0.20	46	F		x	
GMS	CCC	0.20	58	M		x	
ISM	CCC	0.20	39	M		x	
OMG	CCC	0.21	49	M		x	
MAP	CCC	0.23	50	F	x	x	
EPG	CCC	0.23	41	M		x	
JRJ	CCC	0.23	51	M		x	
LRJ	CCC	0.25	66	F		x	
HBO	CCC	0.25	36	M	x	x	x
PMG	CCC	0.29	57	M	x	x	x
ABG	CCC	0.30	64	F		x	
ZMC	CCC	0.36	54	F	x	x	x
JAB	CCC	0.55	41	M		x	
AAF2	CCC	0.64	60	M	x	x	x
JMS	CCC	0.66	50	M		x	
LAL	CCC	0.29	39	M		x	x
EMBT	control		25	M	x	x	
LO	control		46	M	x	x	
ESS	control		22	M	x	x	x
ZFS	control		x	M	x	x	x
FJR	control		28	M	x	x	x
MBFM	control		17	M	x	x	x
3557	control				x	x	

https://doi.org/10.1371/journal.pntd.0008889.t001

inflammation, IFNγ-modulated genes/Th1 response, extracellular matrix, fibrosis, contractility of heart, hypertrophy, arrhythmia, oxidative stress/antioxidant response, and mitochondria-related genes. The number of DEGs for each process is described on **Fig 2B**. **S3 Table** contains the complete list of DEGs belonging to each pathobiological process. As expected, inflammation and IFNγ-dependent/Th1 response processes show the highest number of DEGs (361 and 148, respectively), followed by fibrosis (82) and hypertrophy (53). Of interest, we found a significant number of DEGs belonging to mitochondria and oxidative stress functions/processes (42 and 35, respectively). Some DEGs are shared by several biological functions/processes (**S4 and S5 Tables**). IFNγ-dependent DEGs were found in all other 8 processes, ranging from 9% to 40% of genes in the other processes; those represented 104 inflammation, 33 fibrosis, 18 hypertrophy, 8 contractility and 7 mitochondrial genes.

Among these processes inflammation may be specific to CCC as shown in previous gene expression studies [11,12]. For the other processes, they have been also described in dilated
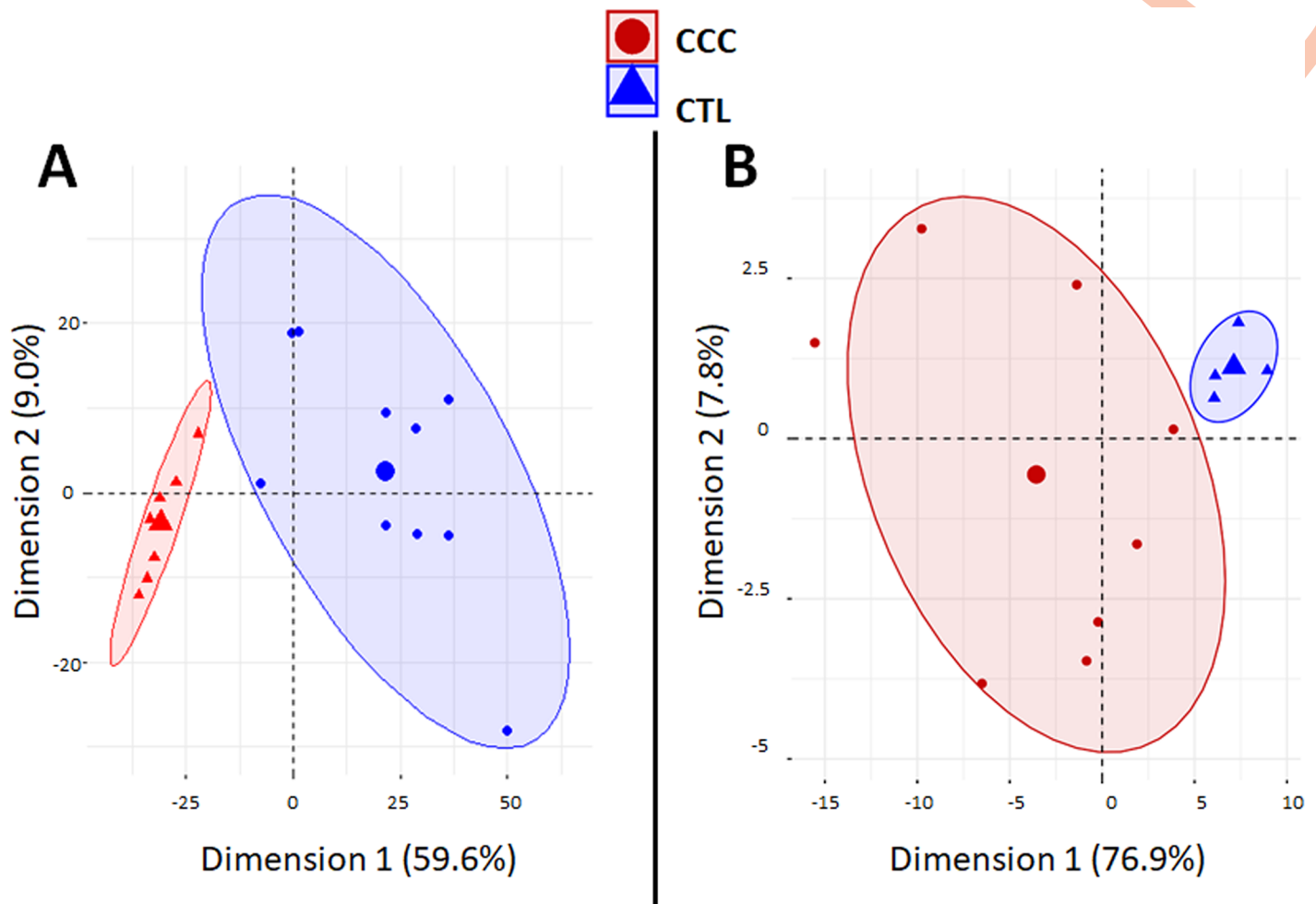
Fig 1. Principal component analysis (PCA) plots. Principal component analysis (PCA) plot of samples was performed based (A) on 1535 differentially expressed genes (DEGs) between CCC and controls. The two main principal components have the largest possible variance (68.8%). The 1535 DEGs had an equal contribution to the first component (ranging from 6.0E-3% to 0.1%). For the second component, 25 DEGs had a contribution over 0.25% (GAB3, WBSCR27, LOC100130930, C1orf35, ISLR2, SLC25A34, NOTCH2, TSPAN32, ATP1A1OS, C11orf65, ZNF214, APCDD1, C1QTNF6, RANBP17, MNS1, APBB3, ANGPTL1, BEND6, LTB, MMP9, ITGB2, PIK3R1, NOTCH2NL, TRMT5 and XLOC_005730); (B) or on 80 differentially expressed miRNAs (DEMs) between CCC and controls. The two main components explain 84.7% of the variance. For the first component, the 80 DEMS had an equal contribution (ranging from 0.24% to1.74%). For the second component, even if all the DEMs contribute, six of the DEMs have a main contribution (hsa-miR-155: 12.8%; hsa-miR-146a: 9.0%; hsa-miR-302d: 8.8%; hsa-miR-378: 8.1%; hsa-miR-486: 7.0%; and hsa-miR-221: 5.2%).

cardiomyopathies of other etiologies. Upstream regulator analysis performed by IPA examines how many targets of each given transcriptional regulator are present in the DEGs—as well as the direction of change–based on the literature and IPA knowledge base; putative regulators are ranked according to overlap with expected targets and directionality (z-score). It indicated that IFNγ is the top upstream regulator, followed by other cytokines like TNFα, IL-18 and EBI3/IL27Rβ chain, the chemokines CCL5 and CXCL10, the transcription factors NF-kB and Ap1, and the PI3K enzyme (**Table 2**). **S6 Table** shows the 27 cytokines and chemokines upregulated in CCC heart tissue. Significantly, the 7 most upregulated among them were chemokines, including chemokine ligands of CCR5 (CCL5, CCL4) and CXCR3 CXCL9 and CXCL10). Multiple cytokines and chemokines that were top upstream regulators like IFNγ, CCL5, CXCL10, IL-18, IL-7, EBI3/IL-27b and IL-4 were found to be upregulated to different degrees in CCC myocardium. Deconvolution of immune cell type profiles in CCC
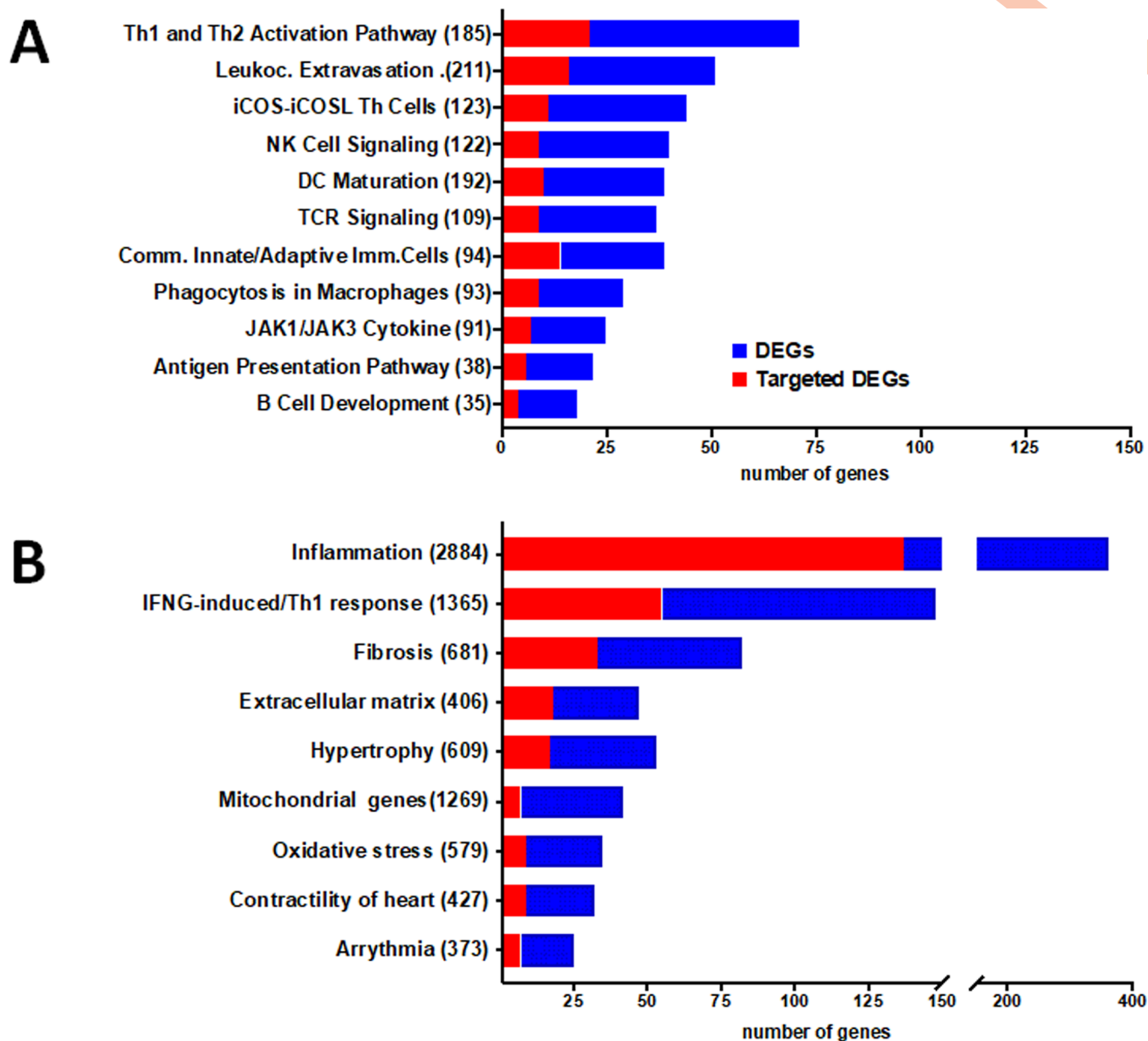
Fig 2. DEGs and DEM-targeted DEGs present in relevant canonical pathways and pathophysiological processes. The stacked bar chart displays the number of DEG (blue) and DEM-targeted DEGs (red) present in each pathway. **A.** Ingenuity Pathway Analysis (IPA) canonical pathways representative of the most significantly enriched in the heart of CCC patients. **B.** DEG and DEM-targeted DEGs in specific biological processes relevant for the CCC pathogenesis. The numerical value in the parentheses in front of each pathway name represents the total number of genes in that pathway/process.

https://doi.org/10.1371/journal.pntd.0008889.g002

myocardium revealed an enrichment of gene expression signatures of CD4+ T cells, NK cells, B cells/plasma cells, dendritic cells, plasmacytoid dendritic cells, regulatory T cells and granulocytes (red; Fig 3). This indicates that these cell types infiltrate the myocardium of CCC patients. Conversely, genes down-regulated in CCC myocardium when compared to controls were enriched with signatures of cardiac muscle cells (blue; Fig 3). This result is most likely a consequence of reduced representation of cardiac mRNAs in CCC myocardium that was replaced by inflammatory cells.

Table 2. Upstream regulator analysis in CCC myocardium.

Upstream Regulator	Molecule	Activation z-score	p-value of overlap
IFNG	cytokine	7.891	2.38E-24
TNF	cytokine	6.494	2.19E-12
IL18	cytokine	4.583	8.95E-14
NFkB (complex)	complex	4.465	5.54E-06
CD40LG	cytokine	4.287	4.10E-15
TCR	complex	3.832	1.80E-26
BCR (complex)	complex	3.771	1.27E-15
IL7	cytokine	3.466	6.32E-18
TET2	enzyme	3.357	4.04E-03
IL4	cytokine	3.082	7.43E-23
EBI3 (IL27Rβ chain IL27RB)	cytokine	2.785	2.13E-05
Fcer1	complex	2.72	3.35E-05
CXCL10	cytokine	2.581	3.15E-04
Ap1	complex	2.454	5.70E-03
CCL5	cytokine	2.432	5.92E-03
U1 snRNP	complex	2.384	1.24E-06
TNFSF14 (LIGHT)	cytokine	2.224	9.77E-03
PI3K (complex)	complex	2.007	3.62E-04
Collagen type I	complex	2.000	3.96E-01

https://doi.org/10.1371/journal.pntd.0008889.t002

Regarding microRNA analysis, it was performed on 8 CCC and 4 control myocardial samples contained in the mRNA transcriptome experiment (10 CCC and 7 control myocardial samples). 754 human miRNAs were screened on the heart samples and among them, 210 miRNAs were detected in every sample; these were quantified in each tissue sample. **S7 Table** shows the expression levels and statistical significance of the 210 expressed miRNAs. Based on their expression values, we have found that 80 out of 210 miRNAs were differentially expressed (DEMs) (absolute FC ≥1.5, p<0.05 without correction). A PCA analysis based on the all differentially expressed miRNAs (**Fig 1B**) and a heatmap (**S1B Fig**) confirmed that miRNA patterns were substantially different from controls. After correction for multiple testing, only miR-146a-000468 (p = 6,9E-03) and miR-155-002623 (p = 6,9E-03) remain significantly altered. However, the list of the 80 miRNAs obtained without correction for multiple testing seems to be relevant as it contains miR-1 (p = 5,0E-03), miR-133a (p = 1,4E-02) and miR-133b (p = 1.3E-2) that we previously observed as under-expressed in CCC samples as compared to controls [28]. MiR-208a, which was also previously described to be under expressed in CCC samples in the same study [28], is borderline in the present study (p = 5,5E-02).

As the controls were younger than CCC we performed some PCA analyses restricted on CCC including DEG information (**S2A Fig**) or DEM information (**S2B Fig**) then we overlaid the age of the patients. No obvious correlation was detected. We performed some spearman correlation tests 9 DEGs were age correlated and none of the DEM were age correlated (**S8 Table**). So, the age may not act as a confounding factor. Similarlly, we did a PCA analysis on cases and controls taking into account DEG information or DEM information and the sex of the patients. No specific clustering was detected (**S3A and S3B Fig**). For each DEG and DEM we made Student's t tests between the male and female patients and no association were detected.

In order to identify putative miRNA-target gene interactions among DEMs and DEGs, we performed inverse expression pairing of DEMs (80) and DEGs (1535). A total of 571 miRNA-
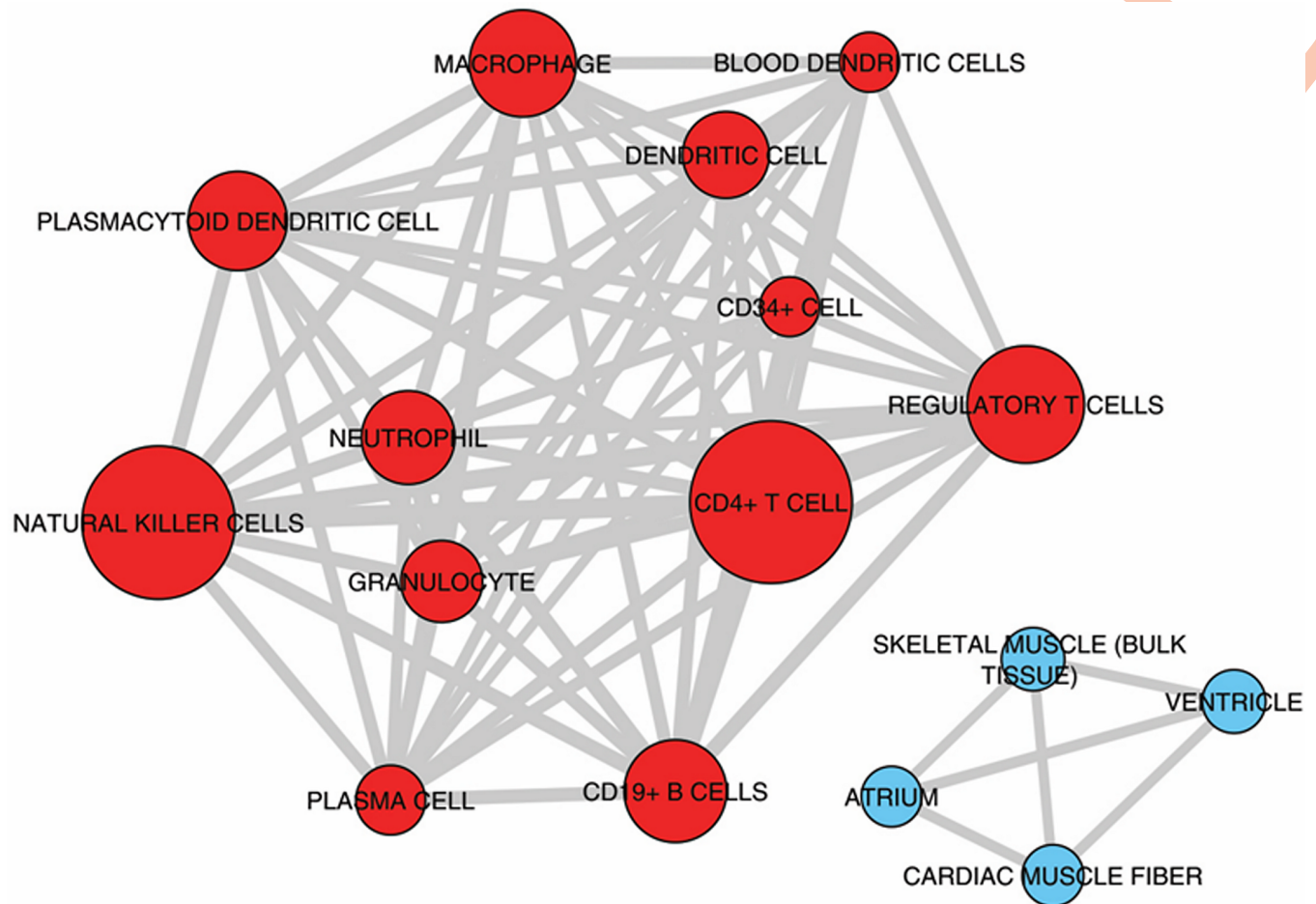
Fig 3. Enrichment analysis of cell subset and tissue signatures. Signatures of different tissues and cell types from ARCHS4 tissue database enriched with up-regulated (red nodes) or down-regulated (blue nodes) genes compared to controls (Adjusted P-value < 0.001). The width of edges (connecting lines) is proportional to the number of genes shared by two signatures. The size of nodes is proportional to the -log10 Adjusted P-value.

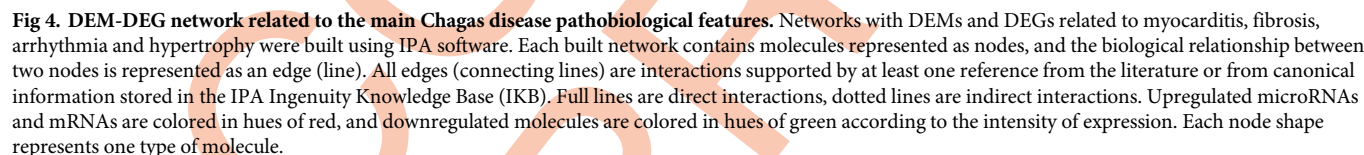https://doi.org/10.1371/journal.pntd.0008889.g003

mRNA interactions involving 67 DEMs and 396 DEGs were found by IPA. **S9 Table** depicts all observed DEM-DEG interactions. **Fig 2A** shows the number of DEGs in the most important canonical pathways and the fraction that is targeted by DEMs. The proportion of DEGs targeted by DEMs in each depicted canonical pathway varies from 24% to 62%. A similar analysis done on DEM-DEG interactions in the 9 key pathobiological processes, which also indicated that a substantial proportion of DEGs (16.7–40.8%) are targeted by DEMs. Apart from the inflammation (38%) and IFNγ-induced genes (37.2%), pathobiological processes with the highest number of DEM-targeted DEGs are fibrosis (40.2%), extracellular matrix (38.2%) and hypertrophy (32.1%) processes (**Fig 2B**). **S10 Table** shows all DEM-DEG interactions classified according to biological process. In order to validate the specificity of the DEM-DEG targeting, we simulated the targeting of the DEGs with 80 miRNAs that were not differentially expressed in CCC myocardium (non-DEMs) as compared to 80 DEMs using the IPA miRNA target filter function, again focusing only high predicted and experimentally observed targets. Comparing the number of target DEGs in the top 6 IPA canonical pathways that were shared by DEMs and non-DEMs, we found a 50% higher number of DEG targets from DEM than DEG targets of the simulated non-DEMs (p<0.00001, chi-square). This suggests that the pairing of DEG targets with DEM was not random.

We found that 5 miRNAs (hsa-miR-125b-5p, hsa-miR-15a-5p, hsa-miR-296-5p, hsa-miR-29c-3p and hsa-miR-103a-3p) each regulate more than twenty DEGs; moreover, each of them affects at least 6 of the 9 biological functions and processes analyzed (S11 Table). Moreover, several of these "master" miRNAs targeted multiple genes belonging to a given process at the same time, suggesting a synergistic action. A network built with DEM-DEG targets around the important pathobiological processes, myocarditis, fibrosis, hypertrophy and arrhythmia disclosed a strong focus on fibrosis, and several miRNAs and targets participated in various processes (summarized on Fig 4). We validated the expression of 38 genes belonging to the four pathobiological processes with real time RTqPCR in a larger set of CCC samples.

Discussion

To assess the role of miRNAs in regulating gene expression in CCC myocardium, we performed an integrative genome-wide analysis of miRNAs and mRNA expression in CCC myocardium samples and performed network and pathways analysis. We identified 1535 differentially expressed genes (DEGs) and 80 differentially expressed miRNAs (DEMs). We found that both miRNAs and mRNA expression profiles discriminated CCC from control samples. Pathways analysis disclosed an enrichment in inflammation, Th1/IFN-γ-inducible genes, genes belonging to fibrosis, hypertrophy, and mitochondrial/oxidative stress/antioxidant response. Our results corroborated that IFN-γ is the key cytokine modulating transcriptional changes in CCC myocardium and affecting all other studied pathobiological processes, and cell type deconvolution indicated the presence of novel immune cell types that had not yet been disclosed by immunohistochemistry. Our data also suggest that a significant number of differentially expressed microRNAs target differentially expressed genes; moreover, a few microRNAs may potentially regulate simultaneously multiple genes in key pathways and pathogenetically relevant processes. Our paper is the first to indicate that miRNAs may play a role in promoting major transcriptome changes in human inflammatory cardiomyopathy.

Our results pointed out IFN-γ is the top gene expression regulator with ca. 10% of DEGs being modulatable by it, in all pathobiological processes. Indeed, several studies have shown a negative impact of IFN-γ on the myocardium, leading to reduced contractility, release of chemokines and increased production of atrial natriuretic factor [40–42]. IFN-γ-induced cardiac fibrosis with increased fibroblast proliferation, production of hyaluronan and metalloproteinases 2 and 9 has also been demonstrated [43–46]. The role of IFN-γ, TNF-α and NF-kB as top upregulators are also in line with data in genetically modified murine models. Mice transgenic to IFN-γ developed a TNF-α-dependent inflammatory dilated cardiomyopathy with fibrosis and heart failure [18], and a very similar phenotype was developed by mice constitutively expressing active IKK2 [47]. Mechanistically, IFN-γ induces TNF-α and potentiates TNF-α-mediated NF-kB signaling and upregulation of NOS2 [48,49], leading to cardiomyocyte contractile dysfunction and apoptosis [Sun, 1998 #110]. This is mediated at least in part by NADPH-and NOS2-dependent production of reactive oxygen and nitrogen species (ROS and RNS, respectively), with oxidative and nitrosative stress [40,50]. IFN-γ -induced RNS leads to inhibition of mitochondrial oxidative metabolism [51] and ATP depletion in cardiomyocytes [52] with ensuing mitochondrial dysfunction. Of interest, 169 DEGs, or ca 10% of DEGS are potentially modulated by NF-kB in CCC myocardium. Our data point towards IFN-γ and NF-kB-mediated signaling as a major player in Chagas cardiomyopathy; we believe they may have a central role in orchestrating the molecular processes that contribute to heart failure. It is noteworthy that IFN-γ may also act through modulation of miRNA expression in CCC myocardium. IFN-γ down-regulates 5 miRNAs (27b, 92a, 99a, 99b, 101) [53,54] which found to be downregulated DEMs in CCC myocardium.

Fig 4. DEM-DEG network related to the main Chagas disease pathobiological features. Networks with DEMs and DEGs related to myocarditis, fibrosis, arrhythmia and hypertrophy were built using IPA software. Each built network contains molecules represented as nodes, and the biological relationship between two nodes is represented as an edge (line). All edges (connecting lines) are interactions supported by at least one reference from the literature or from canonical information stored in the IPA Ingenuity Knowledge Base (IKB). Full lines are direct interactions, dotted lines are indirect interactions. Upregulated microRNAs and mRNAs are colored in hues of red, and downregulated molecules are colored in hues of green according to the intensity of expression. Each node shape represents one type of molecule.

https://doi.org/10.1371/journal.pntd.0008889.g004

Previous immunohistochemistry studies on CCC heart tissue haves identified a few cell types in the inflammatory infiltrate. Most cells were CD68+ macropages, CD4 and CD8+ T cells, with fewer B cells, NK cells, and TGF-beta-expressing cells [7,8,10]. In addition to these cell types, the deconvolution of immune cell type transcriptional profiles shown here provided evidence for the presence of plasmacytoid dentritic cells, regulatory cells, plasma cells and granulocytes. Many of the genes in the NK signature are shared with CD8+ cytotoxic T cells which are abundant in CCC heart tissue [8]; this has previously been observed in transcriptome profiling of peripheral blood from CCC patients [27], and we believe our finding in

myocardium represents an NK/CD8+ T cell cytotoxicity signature. Regarding regulatory T cells, we had previously found a low expression of CTLA-4 mRNA in CCC heart tissue, suggesting a small component of CTLA-4+ T regs [12].

A significant proportion of the DEGs in the pathways and processes we studied (15–62%) were targeted by differentially expressed miRNA (DEM). We found that some DEMs had unusually high numbers of target DEGs. Five downmodulated DEMs (hsa-miR-15a-5p, hsa-miR-29c-3p, hsa-miR-103a-3p, hsa-miR-125b-5p and hsa-miR-296-5p) each targeted at least 20 DEGs involved in 6 or more studied pathobiological processes. Their functions in the context of heart disease and inflammation are described below. Downmodulated miR-15a may targets 23 upregulated DEGs involved in 5 out of the 8 processes described above. Previous data indicate that the miR-15 family is involved in TGFβ-pathway inhibition [55] while miR-15 antagonists induce fibrosis and hypertrophy [56], which are important features of Chagas disease. Our study also revealed down regulation of hsa-miR-29c-3p, associated with 21 upregulated target DEGs involved in all processes described above. The miR-29 family members target several genes related to extracellular matrix and fibrosis [57–59], and miR29b was shown to be inhibited by the myocardial infarction associated transcript (MIAT) [29], a long non-coding RNA overexpressed in CCC patients' myocardium [60].

Downmodulated miR-103 targets 20 upregulated DEGs, involved in 6 out of the 8 processes previously described. MiR-103 is overexpressed in the myocardium of heart failure patients [61], and attenuates cardiomyocyte hypertrophy by a mechanism that partially relies on reducing cardiac autophagy [62]. Down modulated miR-125b targets 23 upregulated DEGs in 6 out of the 8 processes described above. The miR-125 family members negatively regulate the expression of TNF-α, reducing ischemia/reperfusion damage [63] also reducing chemokine RANTES (CCL5), which is highly expressed in our CCC samples. Lastly, down modulated miR-296 targets 22 upregulated DEGs. MiR-296 is linked to fibrosis, and is similarly downregulated in hypertensive patients [64].

Only two miRNAs (miR-155-5p and miR-146a-5p) were found to be upregulated in CCC patients. miR-155 has been shown to increase the global Nrf2 transcriptional response by targeting translation of the transcriptional regulator BACH1 [65], indicating that this miRNA may have an impact on oxidative stress in CCC hearts and its upregulation may have occurred as a compensatory mechanism to intense oxidative stress. This hypothesis will require biological validations. The Nrf2 pathway and HMOX1 have been reported to play a role in "tissue tolerance"—the ability of resist pathogen, inflammation, or oxidative stress-mediated damage during infection or inflammation [66,67] and we have found that HMOX2, a homologous Nrf2-induced gene involved in the antioxidant response, is down regulated in CCC myocardium. miR-146a is expressed in multiple cardiac cell types [68] and was found to be increased upon induction of cardiotoxicity and to inhibit proteins involved in heart regeneration (ErbB-2 and -4) [69,70], suggesting that overexpression of this miRNA may have a negative impact on cardiac function. On the other hand, miR-146a was shown to be induced by NF-κB and to create an anti-inflammatory feedback loop by inhibiting NF-κB-induced proinflammatory cytokine production and inflammatory cell migration into the myocardium [71,72] promoting Treg suppressor function [73], suggesting that this miRNA also presents cardioprotective effects. However, we have shown here and elsewhere [11,12] that Th1 inflammatory cytokines and chemokines are highly expressed in CCC heart tissue and very few Treg are detectable in CCC myocardium [10–12]. Like miR-155, it is possible that it is upregulated as a failed attempt to modulate inflammation.

Our study was performed in whole heart tissue, containing several cell types, including cardiomyocytes, fibroblasts, endothelial and infiltrating inflammatory cells. We must thus keep in mind that results reflect the composite of mRNA and microRNA content of each cell type with

its respective contribution. Most of the RNA will come from cardiomyocytes, but inflammatory cell RNA will readily show up, since control tissue is free from inflammatory infiltrates, showing at most passenger leukocytes that are much less numerous. At any event, our results suggest that, by targeting multiple genes in relevant pathogenic disease pathways and processes, miRNAs can exert a combined regulatory effect that may be stronger than the effect of a single DEM-DEG interaction. In addition, we found a small number of key "high-ranking" differentially expressed miRNAs—those with the highest number of targets, overlapping with those with multiple targets involved in several pathological processes. Our data identified specific molecular features in key pathogenic processes. Further investigation and validation of the more important miRNA-mRNA interactions involved in fibrosis, oxidative stress, and mitochondrial processes may reveal important insights into the pathogenesis of CCC and may translate in the identification of novel therapeutic targets. Our findings may have a bearing on myocarditis and inflammatory cardiomyopathy of distinct etiologies as well as to IFN-γ mediated age-related myocardial inflammation and functional decline [74] as recently described.

Supporting information

S1 Table. List of differentially expressed genes on human heart biopsies from end stage patients or organ donors.
(PDF)

S2 Table. Description of the canonical pathways containing the DEGs in CCC myocardium.
(PDF)

S3 Table. DEGs associated to biological functions and processes in CCC myocardium.
(PDF)

S4 Table. Number of DEGs shared between several pathobiological functions or processes in CCC myocardium.
(PDF)

S5 Table. DEGs shared between several pathobiological functions or processes in CCC myocardium.
(PDF)

S6 Table. Cytokines and chemokines differentially expressed in CCC heart tissue.
(PDF)

S7 Table. DEMs in CCC myocardium.
(PDF)

S8 Table. Correlation between DEG/DEM and the age of the patients.
(PDF)

S9 Table. DEM-DEG interactions in CCC myocardium.
(PDF)

S10 Table. DEM-DEG interaction in each pathobiological function or process in CCC myocardium.
(PDF)

S11 Table. Five DEMs that control a large number of DEGS and processes in CCC myocardium.
(PDF)

S1 Fig. Unsupervised hierarchical clustering done on patients with severe chronic Chagas disease cardiomyopathy (CCC) and controls. A. Unsupervised hierarchical clustering based on the 1535 DEGs. **B.** Unsupervised hierarchical clustering based on the 80 DEMs.
(TIF)

S2 Fig. Principal component analysis (PCA) plots taking into account the age of the cases. Principal component analysis (PCA) plot of samples was performed based **A.** on 1535 differentially expressed genes (DEGs) between CCC and controls. **B.** on 80 differentially expressed miRNAs (DEMs) between CCC and controls. Each plot was generated only on cases and the age of of the patients was overlaid.
(TIF)

S3 Fig. Principal component analysis (PCA) plots taking into account the sex of the cases and controls. Principal component analysis (PCA) plot of samples was performed based **A.** on 1535 differentially expressed genes (DEGs) between CCC and controls. **B.** on 80 differentially expressed miRNAs (DEMs) between CCC and controls. On each plot cases and controls are indicated according to their sex.
(TIF)

Acknowledgments

Author Contributions

Conceptualization: Jorge Kalil, Edecio Cunha-Neto, Christophe Chevillard.

Data curation: Sandrine Cabantous, Amanda Farage Frade, Priscila Camillo Teixeira, Darlan da Silva Cândido.

Formal analysis: Laurie Laugier, Ludmila Rodrigues Pinto Ferreira, Frederico Moraes Ferreira, Sandrine Cabantous, Amanda Farage Frade, Priscila Camillo Teixeira, Darlan da Silva Cândido, Edecio Cunha-Neto, Christophe Chevillard.

Funding acquisition: Jorge Kalil, Edecio Cunha-Neto, Christophe Chevillard.

Investigation: Laurie Laugier, Ludmila Rodrigues Pinto Ferreira, Sandrine Cabantous, Amanda Farage Frade, Priscila Camillo Teixeira, Darlan da Silva Cândido.

Methodology: Laurie Laugier, Ludmila Rodrigues Pinto Ferreira, Sandrine Cabantous, Amanda Farage Frade, Priscila Camillo Teixeira, Darlan da Silva Cândido.

Project administration: Edecio Cunha-Neto, Christophe Chevillard.

Resources: Ronaldo Honorato Barros Santos, Edimar A. Bocchi, Fernando Bacal, Edecio Cunha-Neto.

Software: Frederico Moraes Ferreira, Pauline Brochet, Vanessa Escolano Maso, Helder I. Nakaya.

Supervision: Jorge Kalil, Edecio Cunha-Neto, Christophe Chevillard.

Validation: Pauline Brochet, Vanessa Escolano Maso, Helder I. Nakaya, Edecio Cunha-Neto, Christophe Chevillard.

Visualization: Vanessa Escolano Maso, Helder I. Nakaya, Edecio Cunha-Neto, Christophe Chevillard.

Writing – original draft: Edecio Cunha-Neto, Christophe Chevillard.

Writing – review & editing: Joao Paulo Nunes, Rafael Almeida Ribeiro, Jorge Kalil, Edecio Cunha-Neto, Christophe Chevillard.

References

1. Bocchi EA, Bestetti RB, Scanavacca MI, Cunha Neto E, Issa VS Chronic Chagas Heart Disease Management: From Etiology to Cardiomyopathy Treatment. J Am Coll Cardiol 2017; 70: 1510–1524. https://doi.org/10.1016/j.jacc.2017.08.004 PMID: 28911515

2. Chevillard C, Nunes JPS, Frade AF, Almeida RR, Pandey RP, Nascimento MS et al. Disease Tolerance and Pathogen Resistance Genes May Underlie Trypanosoma cruzi Persistence and Differential Progression to Chagas Disease Cardiomyopathy. Front Immunol 2018; 9: 2791. https://doi.org/10.3389/fimmu.2018.02791 PMID: 30559742

3. Morillo CA, Marin-Neto JA, Avezum A, Sosa-Estani S, Rassi A, Rosas F et al. Randomized Trial of Benznidazole for Chronic Chagas' Cardiomyopathy. N Engl J Med 2015; 373: 1295–1306. https://doi.org/10.1056/NEJMoa1507574 PMID: 26323937

4. Abel LC, Rizzo LV, Ianni B, Albuquerque F, Bacal F, Carrara D et al. Chronic Chagas' disease cardiomyopathy patients display an increased IFN-gamma response to Trypanosoma cruzi infection. J Autoimmun 2001; 17: 99–107. https://doi.org/10.1006/jaut.2001.0523 PMID: 11488642

5. Gomes JA, Bahia-Oliveira LM, Rocha MO, Busek SC, Teixeira MM, Silva JS et al. Type 1 chemokine receptor expression in Chagas' disease correlates with morbidity in cardiac patients. Infect Immun 2005; 73: 7960–7966. https://doi.org/10.1128/IAI.73.12.7960-7966.2005 PMID: 16299288

6. Sousa GR, Gomes JA, Fares RC, Damasio MP, Chaves AT, Ferreira KS et al. Plasma cytokine expression is associated with cardiac morbidity in chagas disease. PLoS One 2014; 9: e87082. https://doi.org/10.1371/journal.pone.0087082 PMID: 24603474

7. Fonseca SG, Reis MM, Coelho V, Nogueira LG, Monteiro SM, Mairena EC et al. Locally produced survival cytokines IL-15 and IL-7 may be associated to the predominance of CD8+ T cells at heart lesions of human chronic Chagas disease cardiomyopathy. Scand J Immunol 2007; 66: 362–371. https://doi.org/10.1111/j.1365-3083.2007.01987.x PMID: 17635814

8. Higuchi Mde L, Gutierrez PS, Aiello VD, Palomino S, Bocchi E, Kalil J et al. Immunohistochemical characterization of infiltrating cells in human chronic chagasic myocarditis: comparison with myocardial rejection process. Virchows Arch A Pathol Anat Histopathol 1993; 423: 157–160. https://doi.org/10.1007/BF01614765 PMID: 7901937

9. Reis MM, Higuchi Mde L, Benvenuti LA, Aiello VD, Gutierrez PS, Bellotti G et al. An in situ quantitative immunohistochemical study of cytokines and IL-2R+ in chronic human chagasic myocarditis: correlation with the presence of myocardial Trypanosoma cruzi antigens. Clin Immunol Immunopathol 1997; 83: 165–172. https://doi.org/10.1006/clin.1997.4335 PMID: 9143377

10. Rocha Rodrigues DB, dos Reis MA, Romano A, Pereira SA, Teixeira Vde P, Totes S Jr et al. In situ expression of regulatory cytokines by heart inflammatory cells in Chagas' disease patients with heart failure. Clin Dev Immunol 2012; 2012: 361730. https://doi.org/10.1155/2012/361730 PMID: 22811738

11. Nogueira LG, Santos RH, Ianni BM, Fiorelli AI, Mairena EC, Benvenuti LA et al. Myocardial chemokine expression and intensity of myocarditis in Chagas cardiomyopathy are controlled by polymorphisms in CXCL9 and CXCL10. PLoS Negl Trop Dis 2012; 6: e1867. https://doi.org/10.1371/journal.pntd.0001867 PMID: 23150742

12. Nogueira LG, Santos RH, Fiorelli AI, Mairena EC, Benvenuti LA, Bocchi EA et al. Myocardial gene expression of T-bet, GATA-3, Ror-gammat, FoxP3, and hallmark cytokines in chronic Chagas disease cardiomyopathy: an essentially unopposed TH1-type response. Mediators Inflamm 2014; 2014: 914326. https://doi.org/10.1155/2014/914326 PMID: 25152568

13. Cunha-Neto E, Coelho V, Guilherme L, Fiorelli A, Stolf N, Kalil J Autoimmunity in Chagas' disease. Identification of cardiac myosin-B13 Trypanosoma cruzi protein crossreactive T cell clones in heart lesions of a chronic Chagas' cardiomyopathy patient. J Clin Invest 1996; 98: 1709–1712. https://doi.org/10.1172/JCI118969 PMID: 8878420

14. Fonseca SG, Moins-Teisserenc H, Clave E, Ianni B, Nunes VL, Mady C et al. Identification of multiple HLA-A*0201-restricted cruzipain and FL-160 CD8+ epitopes recognized by T cells from chronically Trypanosoma cruzi-infected patients. Microbes Infect 2005; 7: 688–697. https://doi.org/10.1016/j.micinf.2005.01.001 PMID: 15848276

15. Cunha-Neto E, Chevillard C Chagas disease cardiomyopathy: immunopathology and genetics. Mediators Inflamm 2014; 2014: 683230. https://doi.org/10.1155/2014/683230 PMID: 25210230

16. Cunha-Neto E, Dzau VJ, Allen PD, Stamatiou D, Benvenutti L, Higuchi ML et al. (2005) Cardiac gene expression profiling provides evidence for cytokinopathy as a molecular mechanism in Chagas' disease cardiomyopathy. Am J Pathol 2005; 167: 305–313. https://doi.org/10.1016/S0002-9440(10)62976-8 PMID: 16049318

17. Reifenberg K, Lehr HA, Torzewski M, Steige G, Wiese E, Küpper I et al. Interferon-gamma induces chronic active myocarditis and cardiomyopathy in transgenic mice. Am J Pathol 2007; 171: 463–472. https://doi.org/10.2353/ajpath.2007.060906 PMID: 17556594

18. Torzewski M, Wenzel P, Kleinert H, Becker C, El-Masri J, Wiese E et al. Chronic inflammatory cardiomyopathy of interferon gamma-overexpressing transgenic mice is mediated by tumor necrosis factor-alpha. Am J Pathol 2012; 180: 73–81. https://doi.org/10.1016/j.ajpath.2011.09.006 PMID: 22051774

19. Kindermann I, Kindermann M, Kandolf R, Klingel K, Bultmann B, Müller T et al. Predictors of outcome in patients with suspected myocarditis. Circulation 2008; 118: 639–648. https://doi.org/10.1161/CIRCULATIONAHA.108.769489 PMID: 18645053

20. Valaperti A Drugs Targeting the Canonical NF-kappaB Pathway to Treat Viral and Autoimmune Myocarditis. Curr Pharm Des 2016; 22: 440–449. https://doi.org/10.2174/1381612822666151222160409 PMID: 26696258

21. Brown DA, Perry JB, Allen ME, Sabbah HN, Stauffer BL, Shaikh SR et al. Expert consensus document: Mitochondrial function as a therapeutic target in heart failure. Nat Rev Cardiol 2017; 14: 238–250. https://doi.org/10.1038/nrcardio.2016.203 PMID: 28004807

22. Pall ML The NO/ONOO-cycle as the central cause of heart failure. Int J Mol Sci 2013; 14: 22274–22330. https://doi.org/10.3390/ijms141122274 PMID: 24232452

23. Teixeira PC, Santos RH, Fiorelli AI, Bilate AM, Benvenuti LA, Stolf NA et al. Selective decrease of components of the creatine kinase system and ATP synthase complex in chronic Chagas disease cardiomyopathy. PLoS Negl Trop Dis 2011; 5: e1205. https://doi.org/10.1371/journal.pntd.0001205 PMID: 21738806

24. Lopez M, Tanowitz HB, Garg NJPathogenesis of Chronic Chagas Disease: Macrophages, Mitochondria, and Oxidative Stress. Curr Clin Microbiol Rep 2018; 5: 45–54. PMID: 29868332

25. Yan B, Wang H, Tan Y, Fu W microRNAs in Cardiovascular Disease: Small Molecules but Big Roles. Curr Top Med Chem 2019; 19: 1918–1947. https://doi.org/10.2174/1568026619666190808160241 PMID: 31393249

26. Rupaimoole R, Slack FJMicroRNA therapeutics: towards a new era for the management of cancer and other diseases. Nat Rev Drug Discov 2017; 16: 203–222. https://doi.org/10.1038/nrd.2016.246 PMID: 28209991

27. Ferreira LRP, Ferreira FM, Laugier L, Cabantous S, Navarro IC, da Silva Candido D et al. Integration of miRNA and gene expression profiles suggest a role for miRNAs in the pathobiological processes of acute Trypanosoma cruzi infection. Sci Rep 2017; 7: 17990. https://doi.org/10.1038/s41598-017-18080-9 PMID: 29269773

28. Ferreira LR, Frade AF, Santos RH, Teixeira PC, Baron MA, Navarro IC et al. MicroRNAs miR-1, miR-133a, miR-133b, miR-208a and miR-208b are dysregulated in Chronic Chagas disease Cardiomyopathy. Int J Cardiol 2014; 175: 409–417. https://doi.org/10.1016/j.ijcard.2014.05.019 PMID: 24910366

29. Zhang J, Chen M, Chen J, Lin S, Cai D, Chen C et al. Long non-coding RNA MIAT acts as a biomarker in diabetic retinopathy by absorbing miR-29b and regulating cell apoptosis. Biosci Rep 2017; 37(2): BSR20170036. https://doi.org/10.1042/BSR20170036 PMID: 28246353

30. Zhu XH, Yuan YX, Rao SL, Wang P LncRNA MIAT enhances cardiac hypertrophy partly through sponging miR-150. Eur Rev Med Pharmacol Sci 2016; 20: 3653–3660. PMID: 27649667

31. Yang Y, Wu J, Wang J A database and functional annotation of NF-κB target genes. Int J Clin Exp Med 2016; 9: 7986–7995.

32. Calvo SE, Clauser KR, Mootha VK MitoCarta2.0: an updated inventory of mammalian mitochondrial proteins. Nucleic Acids Res 2016; 44: D1251–1257. https://doi.org/10.1093/nar/gkv1003 PMID: 26450961

33. Chen EY, Tan CM, Kou Y, Duan Q, Wang Z, Meielles GV et al. Enrichr: interactive and collaborative HTML5 gene list enrichment analysis tool. BMC Bioinformatics 2013; 14: 128. https://doi.org/10.1186/1471-2105-14-128 PMID: 23586463

34. Shannon P, Markiel A, Ozier O, Baliga NS, Wang JT, Ramage D et al. Cytoscape: a software environment for integrated models of biomolecular interaction networks. Genome Res 2003; 13: 2498–2504. https://doi.org/10.1101/gr.1239303 PMID: 14597658

35. Navarro IC, Ferreira FM, Nakaya HI, Baron MA, Vilar-Pereira G, Pereira IR et al. MicroRNA Transcriptome Profiling in Heart of Trypanosoma cruzi-Infected Mice: Parasitological and Cardiological Outcomes. PLoS Negl Trop Dis 2015; 9: e0003828. https://doi.org/10.1371/journal.pntd.0003828 PMID: 26086673

36. Dvinge H, Bertone P HTqPCR: high-throughput analysis and visualization of quantitative real-time PCR data in R. Bioinformatics 2009; 25: 3325–3326. https://doi.org/10.1093/bioinformatics/btp578 PMID: 19808880

37. Kauffmann A, Gentleman R, Huber W arrayQualityMetrics—a bioconductor package for quality assessment of microarray data. Bioinformatics 2009; 25: 415–416. https://doi.org/10.1093/bioinformatics/btn647 PMID: 19106121

38. Ritchie ME, Phipson B, Wu D, Hu Y, Law CW, Shi W et al. limma powers differential expression analyses for RNA-sequencing and microarray studies. Nucleic Acids Res 2015; 43: e47. https://doi.org/10.1093/nar/gkv007 PMID: 25605792

39. Laugier L, Frade AF, Ferreira FM, Baron MA, Teixeira PC, Cabantous S et al. Whole-Genome Cardiac DNA Methylation Fingerprint and Gene Expression Analysis Provide New Insights in the Pathogenesis of Chronic Chagas Disease Cardiomyopathy. Clin Infect Dis 2017; 65: 1103–1111. https://doi.org/10.1093/cid/cix506 PMID: 28575239

40. Chae HJ, Ha KC, Kim DS, Cheung GS, Kwak YG, Kim H-M et al. Catalase protects cardiomyocytes via its inhibition of nitric oxide synthesis. Nitric Oxide 2006; 14: 189–199. https://doi.org/10.1016/j.niox.2005.11.008 PMID: 16403660

41. Patten M, Kramer E, Bunemann J, Wenck C, Thoenes M, Long WC Endotoxin and cytokines alter contractile protein expression in cardiac myocytes in vivo. Pflugers Arch 2001; 442: 920–927. https://doi.org/10.1007/s004240100612 PMID: 11680626

42. Wang Z, Jiang B, Brecher P Selective inhibition of STAT3 phosphorylation by sodium salicylate in cardiac fibroblasts. Biochem Pharmacol 2002; 63: 1197–1207. https://doi.org/10.1016/s0006-2952(02)00853-5 PMID: 11960596

43. Dai B, Cui M, Zhu M, Su WL, Qiu MC, Zhang H STAT1/3 and ERK1/2 synergistically regulate cardiac fibrosis induced by high glucose. Cell Physiol Biochem 2013; 32: 960–971. https://doi.org/10.1159/000354499 PMID: 24107317

44. Wan X, Wen JJ, Koo SJ, Liang LY, Garg NJSIRT1-PGC1alpha-NFkappaB Pathway of Oxidative and Inflammatory Stress during Trypanosoma cruzi Infection: Benefits of SIRT1-Targeted Therapy in Improving Heart Function in Chagas Disease. PLoS Pathog 2016; 12: e1005954. https://doi.org/10.1371/journal.ppat.1005954 PMID: 27764247

45. Wu AJ, Lafrenie RM, Park C, Apinhasmit W, Chen ZJ, Birkedal-Hansen H et al. Modulation of MMP-2 (gelatinase A) and MMP-9 (gelatinase B) by interferon-gamma in a human salivary gland cell line. J Cell Physiol 1997; 171: 117–124. https://doi.org/10.1002/(SICI)1097-4652(199705)171:2<117::AID-JCP1>3.0.CO;2-R PMID: 9130458

46. Levick SP, Goldspink PH Could interferon-gamma be a therapeutic target for treating heart failure? Heart Fail Rev 2014; 19: 227–236. https://doi.org/10.1007/s10741-013-9393-8 PMID: 23589353

47. Maier HJ, Schips TG, Wietelmann A, Kruger M, Brunner C, Sauter M et al. Cardiomyocyte-specific IkappaB kinase (IKK)/NF-kappaB activation induces reversible inflammatory cardiomyopathy and heart failure. Proc Natl Acad Sci U S A 2012; 109: 11794–11799. https://doi.org/10.1073/pnas.1116584109 PMID: 22753500

48. Silva JS, Vespa GN, Cardoso MA, Aliberti JC, Cunha FQTumor necrosis factor alpha mediates resistance to Trypanosoma cruzi infection in mice by inducing nitric oxide production in infected gamma interferon-activated macrophages. Infect Immun 1995; 63: 4862–4867. https://doi.org/10.1128/IAI.63.12.4862-4867.1995 PMID: 7591147

49. Vila-del Sol V, Punzon C, Fresno M IFN-gamma-induced TNF-alpha expression is regulated by interferon regulatory factors 1 and 8 in mouse macrophages. J Immunol 2008; 181: 4461–4470. https://doi.org/10.4049/jimmunol.181.7.4461 PMID: 18802049

50. Cheshire JL, Baldwin AS Jr. Synergistic activation of NF-kappaB by tumor necrosis factor alpha and gamma interferon via enhanced I kappaB alpha degradation and de novo I kappaBbeta degradation. Mol Cell Biol 1997; 17: 6746–6754. https://doi.org/10.1128/mcb.17.11.6746 PMID: 9343439

51. Luss H, Watkins SC, Freeswick PD, Imro AK, Nussler AK, Billiar TR et al. Characterization of inducible nitric oxide synthase expression in endotoxemic rat cardiac myocytes in vivo and following cytokine exposure in vitro. J Mol Cell Cardiol 1995; 27: 2015–2029. https://doi.org/10.1016/0022-2828(95)90023-3 PMID: 8523461

52. Wang D, McMillin JB, Bick R, Buja Response of the neonatal rat cardiomyocyte in culture to energy depletion: effects of cytokines, nitric oxide, and heat shock proteins. Lab Invest 1996; 75: 809–818. PMID: 8973476

53. Reinsbach S, Nazarov PV, Philippidou D, Schmitt M, Wienecke-Baldacchino A, Muller A et al. Dynamic regulation of microRNA expression following interferon-gamma-induced gene transcription. RNA Biol 2012; 9: 978–989. https://doi.org/10.4161/rna.20494 PMID: 22767256

54. Zhao AQ, Xie H, Lin SY, Lei Q, Ren WX, Gao F et al. Interferon-gamma alters the immune-related miRNA expression of microvesicles derived from mesenchymal stem cells. J Huazhong Univ Sci Technolog Med Sci 2017; 37: 179–184. https://doi.org/10.1007/s11596-017-1712-1 PMID: 28397044

55. Tijsen AJ, van der Made I, van den Hoogenhof MM, Wijnen WJ, van Deel ED, De Groot NE et al. The microRNA-15 family inhibits the TGFbeta-pathway in the heart. Cardiovasc Res 2014; 104: 61–71. https://doi.org/10.1093/cvr/cvu184 PMID: 25103110

56. Rawal S, Munasinghe PE, Nagesh PT, Lew JKS, Jones GT, Williams MJA et al. Down-regulation of miR-15a/b accelerates fibrotic remodelling in the Type 2 diabetic human and mouse heart. Clin Sci (Lond) 2017; 131: 847–863. https://doi.org/10.1042/CS20160916 PMID: 28289072

57. Liu Y, Taylor NE, Lu L, Usa K, Cowley AW Jr., Ferreri NR et al. Renal medullary microRNAs in Dahl salt-sensitive rats: miR-29b regulates several collagens and related genes. Hypertension 2010; 55: 974–982. https://doi.org/10.1161/HYPERTENSIONAHA.109.144428 PMID: 20194304

58. Sengupta S, den Boon JA, Chen IH, Newton MA, Stanhope SA, Cheng Y-J et al. MicroRNA 29c is down-regulated in nasopharyngeal carcinomas, up-regulating mRNAs encoding extracellular matrix proteins. Proc Natl Acad Sci U S A 2008; 105: 5874–5878. https://doi.org/10.1073/pnas.0801130105 PMID: 18390668

59. van Rooij E, Sutherland LB, Liu N, Williams AH, McAnally J, Gerard RD et al. A signature pattern of stress-responsive microRNAs that can evoke cardiac hypertrophy and heart failure. Proc Natl Acad Sci U S A 2006; 103: 18255–18260. https://doi.org/10.1073/pnas.0608791103 PMID: 17108080

60. Frade AF, Laugier L, Ferreira LR, Baron MA, Benvenuti LA, Teixeira PC et al. Myocardial Infarction-Associated Transcript, a Long Noncoding RNA, Is Overexpressed During Dilated Cardiomyopathy Due to Chronic Chagas Disease. J Infect Dis 2016; 214: 161–165. https://doi.org/10.1093/infdis/jiw095 PMID: 26951817

61. Ellis KL, Cameron VA, Troughton RW, Frampton CM, Ellmers LJ, Richard AM Circulating microRNAs as candidate markers to distinguish heart failure in breathless patients. Eur J Heart Fail 2013; 15: 1138–1147. https://doi.org/10.1093/eurjhf/hft078 PMID: 23696613

62. Qi H, Ren J, E M, Zhang Q, Cao Y, Ba L et al. MiR-103 inhibiting cardiac hypertrophy through inactivation of myocardial cell autophagy via targeting TRPV3 channel in rat hearts. J Cell Mol Med 2019; 23: 1926–1939. https://doi.org/10.1111/jcmm.14095 PMID: 30604587

63. Wang X, Ha T, Zou J, Ren D, Liu L, Zhang X et al. MicroRNA-125b protects against myocardial ischaemia/reperfusion injury via targeting p53-mediated apoptotic signalling and TRAF6. Cardiovasc Res 2014; 102: 385–395. https://doi.org/10.1093/cvr/cvu044 PMID: 24576954

64. Li S, Zhu J, Zhang W, Chen Y, Zhang K, Popescu LM et al. Signature microRNA expression profile of essential hypertension and its novel link to human cytomegalovirus infection. Circulation 2011; 124: 175–184. https://doi.org/10.1161/CIRCULATIONAHA.110.012237 PMID: 21690488

65. Cheng X, Ku CH, Siow RC Regulation of the Nrf2 antioxidant pathway by microRNAs: New players in micromanaging redox homeostasis. Free Radic Biol Med 2013; 64: 4–11. https://doi.org/10.1016/j.freeradbiomed.2013.07.025 PMID: 23880293

66. Soares MP, Gozzelino R, Weis S Tissue damage control in disease tolerance. Trends Immunol 2014; 35: 483–494. https://doi.org/10.1016/j.it.2014.08.001 PMID: 25182198

67. Soares MP, Ribeiro AM Nrf2 as a master regulator of tissue damage control and disease tolerance to infection. Biochem Soc Trans 2015; 43: 663–668. https://doi.org/10.1042/BST20150054 PMID: 26551709

68. Demkes CJ, van Rooi E MicroRNA-146a as a Regulator of Cardiac Energy Metabolism. Circulation 2017; 136: 762–764. https://doi.org/10.1161/CIRCULATIONAHA.117.029703 PMID: 28827220

69. Bersell K, Arab S, Haring B, Kuhn B Neuregulin1/ErbB4 signaling induces cardiomyocyte proliferation and repair of heart injury. Cell 2009 138: 257–270. https://doi.org/10.1016/j.cell.2009.04.060 PMID: 19632177

70. Horie T, Ono K, Nishi H, Nagao K, Kinoshita M, Watanabe S et al. Acute doxorubicin cardiotoxicity is associated with miR-146a-induced inhibition of the neuregulin-ErbB pathway. Cardiovasc Res 2010; 87: 656–664. https://doi.org/10.1093/cvr/cvq148 PMID: 20495188

71. Gao M, Wang X, Zhang X, Ha T, Ma H, Liu L et al. Attenuation of Cardiac Dysfunction in Polymicrobial Sepsis by MicroRNA-146a Is Mediated via Targeting of IRAK1 and TRAF6 Expression. J Immunol 2015; 195: 672–682. https://doi.org/10.4049/jimmunol.1403155 PMID: 26048146

72. Taganov KD, Boldin MP, Chang KJ, Baltimore D NF-kappaB-dependent induction of microRNA miR-146, an inhibitor targeted to signaling proteins of innate immune responses. Proc Natl Acad Sci U S A 2006; 103: 12481–12486. https://doi.org/10.1073/pnas.0605298103 PMID: 16885212

73. Lu LF, Boldin MP, Chaudhry A, Lin LL, Taganov KD, Hanada T et al. Function of miR-146a in controlling Treg cell-mediated regulation of Th1 responses. Cell 2010; 142: 914–929. https://doi.org/10.1016/j.cell.2010.08.012 PMID: 20850013

74. Ramos GC, van den Berg A, Nunes-Silva V, Weirather J, Peters L, Burkard M et al. Myocardial aging as a T-cell-mediated phenomenon. Proc Natl Acad Sci U S A 2017; 114: E2420–E2429. https://doi.org/10.1073/pnas.1621047114 PMID: 28255084